Geochemistry Geophysics Geosystems G3
AN ELECTRONIC JOURNAL OF THE EARTH SCIENCES
Published by AGU and the Geochemical Society

Technical Brief
Volume 8, Number 6
6 June 2007
Q06003, doi:10.1029/2006GC001531
ISSN: 1525-2027

Observations related to tetrahydrofuran and methane hydrates for laboratory studies of hydrate-bearing sediments

J. Y. Lee, T. S. Yun, and J. C. Santamarina
School of Civil and Environmental Engineering, Georgia Institute of Technology, 790 Atlantic Drive NW, Atlanta, Georgia 30332-0355, USA (jooyong.lee@ce.gatech.edu; taesup.yun@ce.gatech.edu; carlos@ce.gatech.edu)

C. Ruppel
School of Earth and Atmospheric Sciences, Georgia Institute of Technology, Atlanta, Georgia 30332, USA

Now at U.S. Geological Survey, 384 Woods Hole Road, Woods Hole, Massachusetts 02543, USA (cruppel@usgs.gov)

[1] The interaction among water molecules, guest gas molecules, salts, and mineral particles determines the nucleation and growth behavior of gas hydrates in natural sediments. Hydrate of tetrahydrofuran (THF) has long been used for laboratory studies of gas hydrate-bearing sediments to provide close control on hydrate concentrations and to overcome the long formation history of methane hydrate from aqueous phase methane in sediments. Yet differences in the polarizability of THF (polar molecule) compared to methane (nonpolar molecule) raise questions about the suitability of THF as a proxy for methane in the study of hydrate-bearing sediments. From existing data and simple macroscale experiments, we show that despite its polar nature, THF's large molecular size results in low permittivity, prevents it from dissolving precipitated salts, and hinders the solvation of ions on dry mineral surfaces. In addition, the interfacial tension between water and THF hydrate is similar to that between water and methane hydrate. The processes that researchers choose for forming hydrate in sediments in laboratory settings (e.g., from gas, liquid, or ice) and the pore-scale distribution of the hydrate that is produced by each of these processes likely have a more pronounced effect on the measured macroscale properties of hydrate-bearing sediments than do differences between THF and methane hydrates themselves.

Components: 6330 words, 6 figures, 1 table.

Keywords: clathrate; methane; tetrahydrofuran; sediment; clay; salt.

Index Terms: 3004 Marine Geology and Geophysics: Gas and hydrate systems; 5460 Planetary Sciences: Solid Surface Planets: Physical properties of materials; 1012 Geochemistry: Reactions and phase equilibria (3612, 8412).

Received 16 November 2006; **Revised** 16 February 2007; **Accepted** 27 February 2007; **Published** 6 June 2007.

Lee, J. Y., T. S. Yun, J. C. Santamarina, and C. Ruppel (2007), Observations related to tetrahydrofuran and methane hydrates for laboratory studies of hydrate-bearing sediments, *Geochem. Geophys. Geosyst.*, *8*, Q06003, doi:10.1029/2006GC001531.

1. Introduction

[2] Gas hydrate is a crystalline compound consisting of guest gas molecules encaged in water molecules. In nature, gas hydrates occur in the sediments of permafrost regions and continental margins, and methane is the most common guest molecule. The stability of gas hydrate depends on temperature, pressure, salinity, and other factors (e.g., soil characteristics). The difficulty of main-

taining recovered natural samples at in situ temperatures (usually 0 to ~25°C) and fluid pressures (typically 5 to 25 MPa) has been one of the key challenges in studying natural gas hydrate-bearing sediments. At the same time, the analysis of measurements obtained in hydrate-bearing provinces during borehole logging or exploration geophysical surveys (e.g., seismic prospecting) has been limited by the lack of high-quality calibrations of physical properties on synthetic laboratory samples with well-characterized lithology, hydrate saturation, and confining pressures.

[3] Numerous laboratory studies have used sediments containing synthetic gas hydrates to investigate mechanical, thermal, and electromagnetic properties of both pure crystals and hydrate-bearing sediments [*Cameron et al.*, 1990; *Waite et al.*, 2002; *Ebinuma et al.*, 2005; *Priest et al.*, 2005; *Santamarina et al.*, 2005; *Winters et al.*, 2005; *Yun et al.*, 2005, 2007]. Unfortunately, the controlled synthesis of methane hydrate in sediments is challenging owing to methane's low solubility in water and the prolonged time required to form hydrate from aqueous phase methane, which is the way that gas hydrate probably forms in deep sediments that are within (not at the boundaries of) the gas hydrate stability zone [e.g., *Buffett and Zatsepina*, 2000; *Spangenberg et al.*, 2005]. Forming methane hydrate in this way requires a source of methane within the sediment (e.g., microbes) and/or transport of methane via diffusional or advective processes.

[4] Several alternative methods have been proposed to produce methane hydrate-bearing sediments, including flushing methane gas through partially saturated sediments, exploiting preexisting ice cages, and using surfactants to increase the availability of the methane gas in water [*Handa and Stupin*, 1992; *Stern et al.*, 1996; *Zhong and Rogers*, 2000; *Waite et al.*, 2002, 2004; *Lin et al.*, 2004]. Each of these procedures produces different pore scale growth patterns [*Zhong and Rogers*, 2000; *Ebinuma et al.*, 2005; *Spangenberg and Kulenkampff*, 2005] and differences in the macroscale behavior of sediments containing these hydrates [e.g., *Yun et al.*, 2007].

[5] Tetrahydrofuran (C_4H_8O, hereafter THF) has long been used as a substitute for methane in laboratory studies [e.g., *Leaist et al.*, 1982; *Handa*, 1984; *Rueff and Sloan*, 1985]. The main advantage of THF relative to methane is THF's complete miscibility in water, which enables relatively rapid, homogeneous synthesis of THF hydrate in sediments and close control of the hydrate volume fraction. THF hydrate, unlike methane hydrate, also has the advantage of being stable at atmospheric pressure and easily achieved temperatures, making possible the use of standard soil cells and loading frames for laboratory experiments [*Bondarev et al.*, 1996; *Santamarina et al.*, 2005; *Yun et al.*, 2005, 2007]. Finally, because THF hydrate does not dissociate to a gaseous phase, poroelastic complications associated with the formation of highly mobile, compressible gas can be avoided.

[6] In recent years, the use of THF as a proxy for methane in studies of hydrate-bearing sediment properties has also been a source of controversy [*Doyle et al.*, 2004], particularly owing to the polar nature of the THF molecule compared to the nonpolar nature of the methane molecule. This paper examines the differences and similarities between the interactions of methane and THF with water, salt, and mineral grains, the major components of natural sedimentary systems in which gas hydrate occurs.

2. Comparison of Known Properties

[7] The properties of THF and methane molecules, their hydrates, and water ice are compiled in Table 1. We first compare the properties of methane and THF, the hydrate guest molecules (Figure 1). Methane, an alkane, consists of a carbon atom with four attached hydrogens that form a tetrahedral structure. As a cyclic ether, THF has ether oxygen as part of the ring. The THF molecule is ~1.5 times larger than the methane molecule and is completely miscible in water. Methane is a nonpolar molecule (dipole moment of zero), but the dipole moment of THF is as high as that of water. Yet the permittivity of THF is very low relative to water and approaches a value comparable to that for nonpolar fluids.

[8] In terms of hydrate properties, THF hydrate forms as Structure II, with THF filling only large cavities. In contrast, methane hydrate most commonly occurs as Structure I with methane filling both large and small cavities. Despite these structural differences, a comparison of the macroscale mechanical and electrical properties and some thermal properties (e.g., heat capacity, thermal conductivity) of the two hydrates reveals gross similarities (Table 1), particularly when each property is considered within the range of values attained in marine or permafrost sediments. On the other hand, there are important differences in thermal expansivity, the heat of dissociation, and

Table 1. Properties of Methane and THF, Their Hydrates, and Water Ice

Property	Methane	Tetrahydrofuran (THF)	Water Ice
	Properties of Guest Molecule		
Molecular formula	CH_4	C_4H_8O	H_2O
Chemical structure	see Figure 1	see Figure 1	see Figure 1
Molecular size, Å	4.36 (1)[a]	6.3 (2)	~1.8 (1)
Dipole moment, D	0 (3)	1.63 (4)	1.85 (3)
Molecular polarizability, $Å^3$	2.6 (5)	7.9 (6)	1.5 (5)
Permittivity	1.7 (7)	7.5 (4)	80 (3)
Density, kg m^{-3}, at 293.5 K	N/A	888 (4)	1000 (3)
Viscosity, cP, at 298.5 K	N/A	0.46 (4)	0.89 (3)
Surface tension, N m^{-1}, at 293.5 K	0.00676 at 140K (8)	0.028 (4)	0.0728 (3)
Solubility in water at 293.5 K	0.04×10^{-3} [mole fraction] (9)	miscible (7)	N/A
	General Characteristics		
Hydrate structure	I	II	n/a
Hydrate cavity diameter, Å	7.9, 8.66 (1)	7.82, 9.46 (1)	n/a
Ideal hydrate stoichiometric ratio	$CH_4.6H_2O$	$C_4H_8O.17H_2O$	n/a
Slope of phase transformation boundary at 10 MPa, K MPa^{-1}	+0.96 (1)	−0.08 (10)	−0.01 (11)
	Thermal Properties of the Frozen State		
Heat capacity, kJ kg^{-1} K^{-1}, at 270 K	2.07 (12)	2.07 (13)	2.10 (13)
Heat of dissociation, kJ kg^{-1}, at 273 K	338.7 (12)	262.9 (13)	333.5 (14)
Thermal conductivity, W m^{-1} K^{-1}	0.5 @ 270 K (15)	0.5 @ 270 K (16)	2.2 @ 263 K (1)
Thermal diffusivity, m^2 s^{-1}	3×10^{-7} @ 270 K (15)	2.8×10^{-7} @ 270 K (17)	8.43×10^{-7} @ 273 K (18)
Thermal linear expansivity, K^{-1}, at 200 K	77×10^{-6} (1)	52×10^{-6} (1)	56×10^{-6} (1)
	Mechanical Properties of the Frozen State		
Density, kg m^{-3}, at 273 K	910 (1)	~910 (1)	917 (1)
Interfacial Tension, J m^{-2}	0.017 (19) −0.032 (20)	0.016–0.031 (21)	0.029 (19) −0.032 (20)
Adiabatic bulk compressibility, Pa, at 273 K	$\sim 14 \times 10^{-11}$ (1)	$\sim 14 \times 10^{-11}$ (1)	12×10^{-11} (1)
Isothermal Young's modulus, Pa, at 268 K	$\sim 8.4 \times 10^9$ (1)	$\sim 8.2 \times 10^9$ (1)	9.5×10^9 (1)
Shear wave speed V_s, m s^{-1}	1950 (22)	1890 (23)	1950 (24) ~1990 (25)
Compressional wave speed V_p, m s^{-1}	3370 (23) ~ 3800 (22)	3670 (23)	3890 (24) ~3910 (25)
Strength, MPa	2 to 10 (26)	0.9 to 44 (27)	0.6 to 1 (26)
	Electrical Properties of Frozen State		
Electrical conductivity, S/m	~0.01 (28)	0.01	0.01 (29)
Dielectric constant at 273 K	~2.5 (28)	4.3	2.8 (29)

[a] The number in parentheses corresponds to the following reference or other source information: 1, *Sloan* [1998]; 2, *Dyadin et al.* [1999]; 3, *Lide* [2003]; 4, *Smallwood* [1996]; 5, *Atkins* [1978]; 6, *Davidson et al.* [1986]; 7, *Carey* [1987]; 8, *Upstill and Evans* [1977]; (9) at 0.1 MPa and 278.15 K from *Handa* [1990]; 10, *Circone et al.* [2003]; 11, *Florusse et al.* [2004]; 12, *Handa* [1986]; 13, *Handa et al.* [1984]; 14, *Petrenko and Whitworth* [1999]; 15, *deMartin* [2001]; 16, *Ross et al.* [1981]; 17, thermal diffusivity of tetrahydrofuran hydrate is estimated from published thermal conductivity and heat capacity values; 18, *Hobbs* [1974]; 19, *Uchida et al.* [2002]; 20, *Anderson et al.* [2003]; 21, estimated from data of *Zakrzewski and Handa* [1993] assuming cylindrical and spherical geometry; 22, *Helgerud et al.* [2003b]; 23, *Kiefte et al.* [1985]; 24, *Helgerud et al.* [2003a]; 25, *Gagnon et al.* [1987]; 26, at 50 MPa confining pressure and 270 K for methane hydrate and the same confining pressure and 260 K for ice, from *Durham et al.* [2005]; 27, measured with no confinement and at 276 K by *Ohmura et al.* [2002]; 28, *Galashev et al.* [2006]; 29, *Shi et al.* [2005].

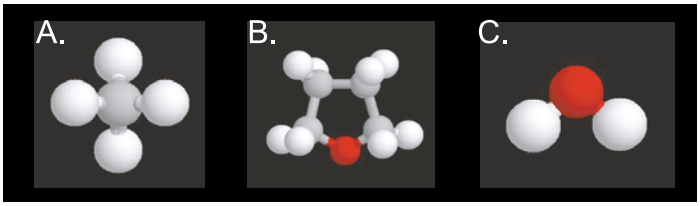

Figure 1. Ball-and-stick representations of the molecular structure of (a) methane (CH_4), (b) tetrahydrofuran (C_4H_8O), and (c) water (H_2O). Oxygen atoms are red, hydrogen are white, and carbon are gray.

the degree to which equilibrium temperature depends on pressure for the two hydrates.

3. Dipole Moment Effects

[9] The polar nature of the THF molecule (relatively large dipole moment) compared to the nonpolar methane molecule has led to concerns about the potential interaction of THF with water and THF hydrate with sediments. We next discuss each of these issues in detail.

3.1. THF-Water Interaction

[10] As mentioned above, the dipole moment of the THF molecule is similar to that of water, but its permittivity is much smaller. The molecular dipole moment μ [Debye = C · m] is determined by the geometric arrangement of charges in a molecule while the permittivity is a measure of macroscale polarizability per unit volume [*Santamarina et al.*, 2001]. The orientational polarization P [C m^{-2}] reflects μ and the number of molecules per unit volume N, as well as the competing effects between the externally imposed electric field E [N C^{-1}] and the randomizing thermal motion at temperature T [K]. The relationship among these parameters is captured in [*Atkins*, 1978]

$$P = \frac{N\mu^2}{3kT}E = \varepsilon_o(\kappa' - 1)E, \qquad (1)$$

where k is Boltzmann's constant [1.38 × 10^{-23} J K^{-1}], ε_o is the permittivity of free space [8.854 × 10^{-12} F m^{-1}], and κ' is the relative permittivity. The permittivities of water and THF are related as

$$\frac{\kappa'_{water} - 1}{\kappa'_{THF} - 1} = \frac{P_{water}}{P_{THF}} = \frac{N_{water}\,\mu_{water}{}^2}{N_{THF}\,\mu_{THF}{}^2}. \qquad (2)$$

Using values from Table 1, the polarization ratio is $P_{water}/P_{THF} \cong 11$, which is similar to the ratio of measured permittivities $(\kappa'_{water} - 1)/(\kappa'_{THF} - 1) = 12$, as shown for microwave complex permittivity spectra in Figure 2. Therefore molecular size, which is captured by N in (1), must be considered in conjunction with the molecular dipole moment for the analysis of the macroscale behavior of THF.

[11] Hydrogen bonds between water molecules are responsible for the interaction between water and other fluids (e.g., THF) and for the activity of water, which is closely related to phase equilibrium conditions [*Luck*, 1973]. Among organic compounds, alcohol and ether form hydrogen bonds with water, which explains the high miscibility of these fluids. As a cyclic ether, the oxygen of a THF molecule uses one of its unshared electron pairs to accept a proton from a water molecule to form a hydrogen bond [*Carey*, 1987]. However, the interaction between THF and water molecules is relatively weak compared to water-water interaction, and water clusters formed by the hydrogen-bonded

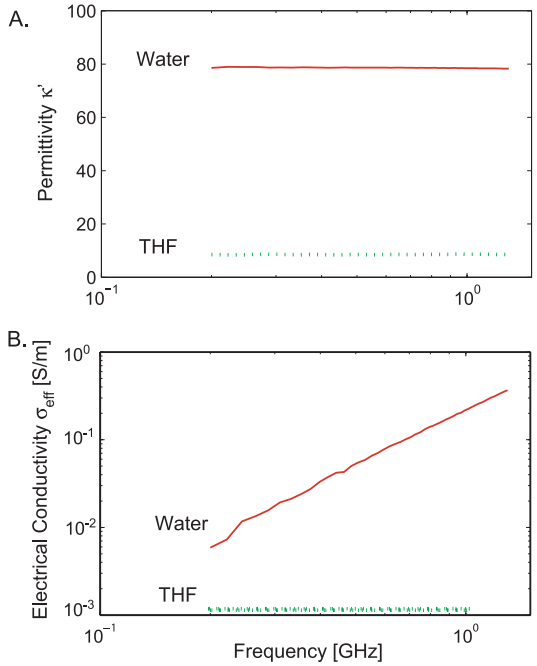

Figure 2. Frequency-dependent electrical properties of liquid water (red) and liquid THF (green): (a) permittivity and (b) electrical conductivity. The conductivity of THF is below the detection limit for the instrumentation.

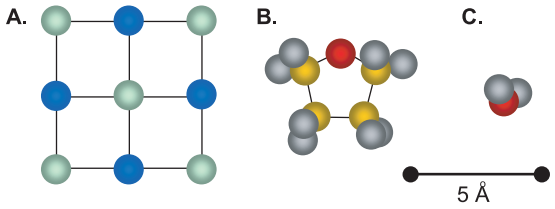

Figure 3. Ball-and-stick representation showing the relative sizes of the (a) sodium chloride; (b) tetrahydrofuran; and (c) water molecules, with interatomic distances on the same absolute scale for the different molecules. Color scheme: green, chloride; blue, sodium; gray, oxygen; red, hydrogen; yellow, carbon.

water network are preserved around THF molecules [*Fukasawa et al.*, 2004; *Ohtake et al.*, 2005; *Takamuku et al.*, 2003]. Thus THF's capacity to form hydrogen bonds does not play a crucial role in hydrate formation, and THF molecules essentially behave as nonpolar molecules.

3.2. Fluid-Salt Interaction

[12] Salts are often present in natural systems as precipitates in sediments or in a dissolved phase in pore fluids. Polar solvents like water can dissolve ionic compounds through thermal agitation and ion-dipole interactions, even though the ion-dipole interaction is weaker than ion-ion interaction. The dissolution of salts by water starts with the alignment of the polar water molecules near ions, with H-ends toward anions and O-ends toward cations. The small water molecules gradually position themselves between surface anions and cations, weaken the ion-ion attraction forces, and eventually pull ions away from the crystal. This sequence of events shows the relevance of polarity and molecular size for the ability of a fluid to dissolve salt. For reference, Figure 3 illustrates the relative sizes of the sodium chloride, tetrahydrofuran, and water molecules.

[13] A key question is whether fluids that contain large polar molecules (e.g., THF) can also dissolve salt. We devised a simple, yet robust, experiment to evaluate the effect of molecular polarity and size on the ability of a fluid to dissolve salt. Three fluids were considered for the study of salt-fluid interactions: water (small polar molecule, high permittivity), THF (large polar molecule, low permittivity), and benzene (nonpolar molecule, low permittivity). The relevant properties of benzene are molecular size of 5.36 Å, zero dipole moment, molecular polarizability of 10.32 $Å^3$, permittivity of 2.28, density of 879 kg m^{-3} at 293.5 K, viscosity of 0.65 cp at 298.5 K, surface tension of 0.0289 N m^{-1} at 293.5 K, and solubility of 0.18 (mole fraction) in water at 293.5 K [*Atkins*, 1978; *Smallwood*, 1996; *Yoshida et al.*, 2005].

[14] Table salt (7g of NaCl) was thoroughly mixed in 50 ml of each liquid. The mixture was then filtered through P5 (5–10 μm) filter paper, and the retained salt was oven-dried and weighed. Within the precision of these measurements, the results show that THF ($\kappa' = 7.52$) and benzene ($\kappa' = 2.28$) do not dissolve NaCl (>99% of the salt retained in solid form) while water ($\kappa' = 80$) dissolves NaCl completely (no salt retained).

[15] Under the microscope, the salt crystals that had been mixed with benzene had intact crystal surfaces (Figure 4b), indicating that the benzene did not react with the salt. The crystal surfaces of the salt mixed with THF showed flakes of precipitated butylated hydroxytoluene (BHT, $C_{15}H_{24}O$), which is added to THF at 0.2g/L to prevent peroxide formation during storage (Figure 4c), but revealed no indication of dissolution. To confirm whether the observed flakes were BHT, the same experiment was repeated with excess BHT (250 g/L) added to the THF, producing extensive BHT precipitation on salt grains (Figure 4d).

[16] These results suggest that the case of dispersed ions surrounded by oriented THF molecules is not entropically favored over a salt crystal surrounded by randomly oriented THF molecules. Yet, while THF cannot dissolve ionic crystalline compounds like salt, there is evidence that THF can solvate pre-existing free ions [*Nishinaga et al.*, 2003]. This implies ion-dipole interaction that is much weaker than the ion-ion interaction in the salt crystal, yet possibly stronger than the Debye interaction of ion to polarized molecule in the case of free ions and methane.

3.3. Fluid-Mineral Interaction

[17] Understanding the interaction of fluids with mineral surfaces is critical for the study of hydrate-bearing sediments. Hence we extended the previous experiments to examine the solvation of ions on dry minerals by the three selected fluids.

[18] Charged mineral particles and absorbed ions near mineral surfaces lower the activity of water [*Hobbs*, 1974]. The formation of electrical double layers on mineral surfaces reflects the balance between the thermal activity and the electrical forces that develop among fluids, ions, and charged mineral surfaces. The characteristic scale of the

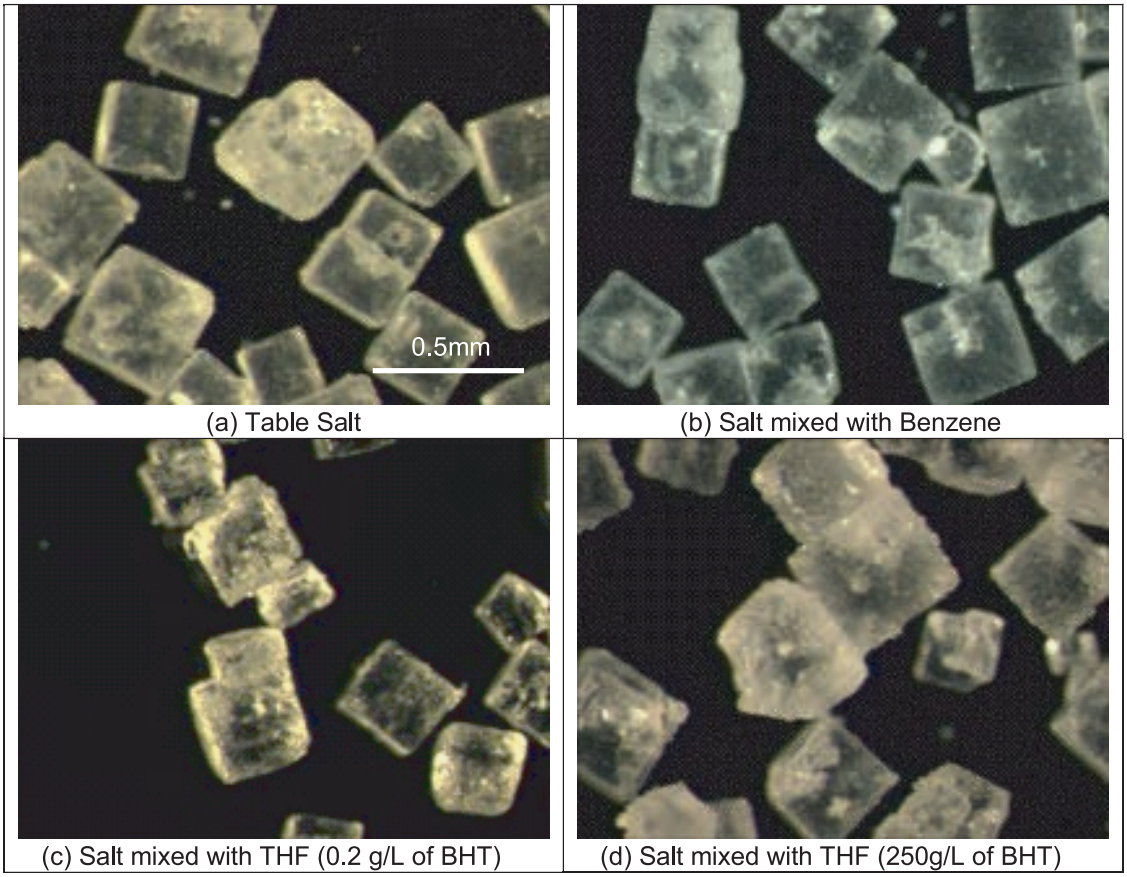

Figure 4. Optical microphotographs of NaCl salt: (a) oven-dried, (b) mixed with benzene and oven-dried; (c) mixed with THF and oven-dried; and (d) mixed with THF with excess BHT and oven-dried.

double layer is determined by the ionic concentration of pore fluids c_o [mol m^{-3}], ionic valence z, temperature T [K], and permittivity κ' [*Mitchell and Soga*, 2005]. The thickness of a double layer is

$$\theta = \sqrt{\frac{\varepsilon_0 k}{2e_0{}^2 N_{av}} \frac{\kappa' T}{c_0 z^2}}, \quad (3)$$

where N_{av} is Avogadro's number [$6.022 \cdot 10^{23}$ mol^{-1}] and e_0 is the elementary charge [1.602×10^{-19} C]. Thicker double layers imply higher interparticle repulsion forces for a given interparticle distance and lower probability of particle aggregation by van der Waals attraction [*Santamarina et al.*, 2001].

[19] We investigated the interaction between each of the three fluids and mineral surfaces using two indirect experimental methods. The first was a sedimentation test, a low solid-fraction experiment that provides insight into incipient fabric formation. The second is the standardized liquid limit test, which is a high solid-fraction experiment frequently used in geotechnical testing to elucidate the effect of the pore fluid character on the interaction among mineral particles in sediments. Both tests were run with bentonite because of its high specific surface (226 m^2 g^{-1}). Particle-to-particle interactions in high specific surface substances are controlled by electrical forces, which in turn reflect fluid-mineral interaction.

3.3.1. Sedimentation

[20] Particle-fluid interaction can be inferred from the settling behavior of sediment suspensions. While Stokes sedimentation of single particles is controlled by particle size and fluid viscosity, the sedimentation of suspensions composed of submicron-sized particles such as bentonite is governed by electrical interparticle forces.

[21] Bentonite (2.5 g) was thoroughly mixed with each fluid (50 ml) in graduated cylinders, and then left to rest. The height of the suspension-water interface and sedimentation characteristics were monitored with time, as shown in Figure 5. Sedi-

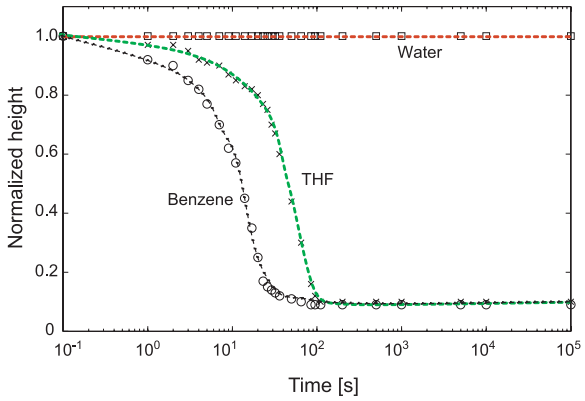

Figure 5. Sedimentation curves for water-bentonite (black), THF-bentonite (green), and benzene-bentonite (red) mixtures.

mentation ended within 10^2 s in benzene and in THF, with only a few fine particles remaining in suspension for longer time in THF. In contrast, bentonite remained suspended in water even after 10^6 s.

[22] Using the evaluation criteria of *Palomino and Santamarina* [2005], the observed sedimentation behavior clearly contrasts dispersed sedimentation in water with aggregated sedimentation in THF and benzene. In water, the suspended particles are dispersed due to the large double layer repulsive forces between particles. In THF and benzene, unsolvated, adsorbed ions shield the clay charge, van der Waals attraction prevails, and particle aggregation occurs followed by fast sedimentation. These results indicate that despite the polar nature of the THF molecule, its interaction with minerals and its ability to solvate ions on mineral surfaces resemble those of nonpolar molecules such as benzene.

3.3.2. Liquid Limit

[23] The liquid limit test is used to determine the water content associated with changes in the rheological behavior of a paste from that of a viscous liquid to a plastic solid. The liquid limit is affected by the specific surface of particles, fluid-mineral interaction, and the resulting soil fabric. High specific surface, thick double layers, and flocculated fabrics lead to higher liquid limits.

[24] The liquid limit of bentonite mixed with each of the three liquids was determined using the standardized fall cone test, which consists of a free-falling stainless steel 80 g cone with a 30° apex into the specimen [*British Standards Institute*, 1990]. The cone is released at the soil surface and penetrates the soil paste until it comes to rest. The test is repeated for different fluid mass fractions. The liquid limit is the fluid content at which the cone penetrates 20 mm.

[25] As shown in Figure 6, small changes in fluid content produced large variations in cone penetration depth when mixtures were prepared with either THF or benzene. The results for water, THF, and benzene were 302%, 69%, and 57%, respectively. This confirms the nonpolar, benzene-like interaction between THF and bentonite.

[26] The soil-fluid pastes were oven-dried after the liquid limit tests, and the cohesiveness of the dried specimens was assessed by indenting them with a blade. The dried water-bentonite mixture was strong and behaved like stiff cemented soil, whereas the dried THF-bentonite mixture maintained its shape but readily crumbled into powder when disturbed. The dried benzene-bentonite mixture had changed back to powder. The cohesiveness of the oven-dried water-bentonite paste suggests that ionic bonding had developed between particles by sharing of dissolved ions while in wet conditions. On the other hand, the slight bonding that remains in the dried THF-bentonite paste might reflect minor interaction among THF, ions, and mineral surfaces, or more likely, the contribution of the precipitated BHT.

[27] Overall, the evaluation of sedimentation characteristics, liquid limits, and dry paste strengths for the bentonite-liquid mixtures confirms that the interaction of THF with fine particles much more closely resembles that of benzene (nonpolar) than that of water (polar). These observations support

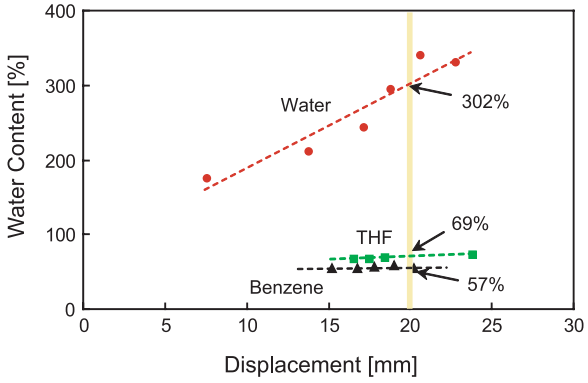

Figure 6. Fall cone penetration lines for water-bentonite (red), bentonite-THF (green), and bentonite-benzene (black) mixtures. The vertical yellow line indicates the displacement (20 mm) at which liquid limit is assessed.

the contention that THF behaves like methane (nonpolar) in the presence of sediment particles.

4. Hydrate Formation in Sediments

[28] After nucleation, the evolution of gas hydrate in porous media is prescribed by the Young-Laplace and the Gibbs-Thompson equations [*Clennell et al.*, 1999]. Within experimental variability, the interfacial tension between hydrate and water is similar for both THF and methane hydrate (Table 1), implying that similar growth patterns should be expected in water-saturated sediments. Beyond these similarities, guest molecules and cavity types can affect mechanical properties of hydrate-bearing sediments [*Durham et al.*, 2005]. In practice, though, factors such as thermodynamic parameters (e.g., cooling rate, diffusion rate for heat of transformation and excluded ions, and, for methane hydrate, the rate of guest molecule diffusion) and the spatial distribution of hydrate in the pore space have a greater impact on measured mechanical properties.

[29] The distribution of hydrates in pore space depends strongly on hydrate formation history. For example, water in partially saturated sediments tends to accumulate near contacts (pendular regime); therefore flooding with gas to trigger hydrate formation [e.g., *Handa and Stupin*, 1992] in such a system leads to preferential hydrate formation at contacts [*Waite et al.*, 2004; *Winters et al.*, 2004; *Ebinuma et al.*, 2005; *Masui et al.*, 2005]. The version of the ice seed method used by *Priest et al.* [2005] involves the introduction of ice and melt prior to pressurizing, making it close to the unsaturated method, and produces a similar effect. On the other hand, the *Stern et al.* [1996] ice-seeding method causes hydrate to preferentially replace ice [*Ebinuma et al.*, 2005] in pore space, even though water from melting ice may also migrate to grain contacts if hydrate formation takes place at a rate lower than ice melting [*Valiullin and Furo*, 2002; *Priest et al.*, 2005]. In contrast, THF hydrate forms from the combination of dissolved THF molecules and water molecules, much as methane hydrate probably forms in deep sediments under natural conditions [*Buffett and Zatsepina*, 2000]. Previous studies with THF hydrate in water-saturated porous media suggest that nucleation occurs at particle surfaces and that hydrate crystals then grow into the pore space [*Yun et al.*, 2005].

[30] The differences in the spatial distribution of hydrates induced by different formation histories affect the stiffness and strength of sediments as well as the bulk conduction properties. For example, the small-strain stiffness and shear strength increase dramatically even with small hydrate saturations in sediments in which hydrate is synthesized by gas flooding sediments with initially low water saturation [*Waite et al.*, 2004; *Winters et al.*, 2004]. From the discussion above, the ice-seeding method produces different results depending on its implementation [*Ebinuma et al.*, 2005; *Masui et al.*, 2005; *Priest et al.*, 2005]. The small-strain stiffness does not increase significantly at low hydrate concentration in sediments when hydrate is synthesized by flushing water containing aqueous phase methane [*Spangenberg and Kulenkampff*, 2005] through initially saturated sediments or by forming hydrate from dissolved THF [*Yun et al.*, 2005, 2007]. Thus it appears that the hydrate formation method is likely more important than the hydrate former in controlling some of the properties of the hydrate-bearing sediment.

5. Conclusions

[31] Despite a dipole moment close to that of water, THF has permittivity as low as that of nonpolar molecules owing primarily to the large size of the molecule. In turn, molecular size hinders THF from hydrating salts or mineral surfaces; therefore the overall behavior of THF in sediments resembles that of a nonpolar fluid. The fact that THF is a polar molecule while methane is not appears to have little relevance for assessing the differences between sediments containing THF hydrate versus those containing methane hydrate.

[32] Despite its polar nature, THF forms weaker hydrogen bonds with water than the water molecules form with each other, meaning that THF has only limited impact on the hydrogen-bonded water network. The available data also indicate that the interfacial tension, a factor important in hydrate growth in pore space, between water and either THF or methane hydrate is similar.

[33] Laboratory formation history and ensuing pore-scale spatial distribution likely have a more pronounced effect on the macroscale mechanical properties of hydrate-bearing sediments than differences between THF and methane hydrates themselves. Nevertheless, the analysis of results gathered with THF hydrate-bearing sediments as a proxy for methane hydrate-bearing sediments should still take into consideration the inherent differences

between these hydrates, particularly with regard to kinetics.

Acknowledgments

[34] This research was sponsored by Goizueta Foundation support to J.C.S. and by a contract to C.R. and J.C.S. from the Joint Industry Project for Methane Hydrate, administered by ChevronTexaco with funding from award DE-FC26-01NT41330 from DOE's National Energy Technology Laboratory. We thank J. Nimblett for compiling an early version of Table 1. C.R. was on assignment at and wholly supported by the U.S. National Science Foundation (NSF) during completion of this work, and the views represented here are those of the authors, not NSF or DOE.

References

Anderson, R., M. Llamedo, B. Tohidi, and R. W. Burgass (2003), Experimental measurement of methane and carbon dioxide clathrate hydrate equilibria in mesoporous silica, *J. Phys. Chem. B*, *107*, 3507–3514.

Atkins, P. W. (1978), *Physical Chemistry*, 1018 pp., W. H. Freeman, New York.

Bondarev, E. A., A. G. Groisman, and A. Z. Savvin (1996), Porous medium effect on phase equilibrium of tetrahydrofuran hydrate, in *Proceedings of the Second International Conference on Natural Gas Hydrates*, pp. 89–93, Toulouse, France.

British Standards Institute (1990), Methods of testing soils for civil engineering purposes, *Br. Stand. 1377–2*, London, U. K.

Buffett, B. A., and O. Y. Zatsepina (2000), Formation of gas hydrate from dissolved gas in natural porous media, *Mar. Geol.*, *164*, 69–77.

Cameron, I., Y. P. Handa, and T. H. W. Baker (1990), Compressive strength and creep-behavior of hydrate-consolidated sand, *Can. Geotech. J.*, *27*, 255–258.

Carey, F. A. (1987), *Organic Chemistry*, 1219 pp., McGraw-Hill, New York.

Circone, S., L. Stern, S. H. Kirby, W. B. Durham, B. C. Chakoumakos, C. J. Rawn, A. J. Rondinone, and Y. Ishii (2003), CO_2 hydrate: Synthesis, composition, structure, dissociation behavior, and a comparison to structure I CH_4 hydrate, *J. Phys. Chem. B*, *107*, 5529–5539.

Clennell, B. M., M. Hovland, J. S. Booth, P. Henry, and W. J. Winters (1999), Formation of natural gas hydrates in marine sediments: 1. Conceptual model of gas hydrate growth conditioned by host sediment properties, *J. Geophys. Res.*, *104*, 22,985–23,003.

Davidson, D. W., R. N. O'Brien, P. Saville, and S. Visaisouk (1986), Optical refraction by clathrate hydrates, *J. Opt. Soc. Am. B Opt. Phys.*, *3*, 864–866.

deMartin, B. J. (2001), Laboratory measurements of the thermal conductivity and thermal diffusivity of methane hydrate at simulated in situ conditions, M.S. thesis, Ga. Inst. of Technol., Atlanta.

Doyle, E. H., et al. (2004), *Charting the Future of Methane Hydrate Research in the United States*, 192 pp., Natl. Acad. Press, Washington, D. C.

Durham, W. B., L. A. Stern, S. H. Kirby, and S. Circone (2005), Rheological comparisons and structural imaging of sI and sII endmember gas hydrates and hydrate/sediment aggregates, in *Proceedings of Fifth International Conference on Gas Hydrates*, *Pap. 2030*, pp. 607–614, Tapir Acad., Trondheim, Norway.

Dyadin, Y. A., E. G. Larionov, A. Y. Manakov, and F. V. Zhurko (1999), Double clathrate hydrate of tetrahydrofuran and xenon at pressures up to 15 kbar, *Mendeleev Commun.*, *2*, 80–81.

Ebinuma, T., Y. Kamata, H. Minagawa, R. Ohmura, J. Nagao, and H. Narita (2005), Mechanical properties of sandy sediment containing methane hydrate, in *Proceedings of Fifth International Conference on Gas Hydrates*, *Pap. 3037*, pp. 958–961, Tapir Acad., Trondheim, Norway.

Florusse, L. J., C. J. Peters, J. Schoonman, K. C. Hester, C. A. Koh, S. F. Dec, K. N. Marsh, and E. D. Sloan (2004), Stable low-pressure hydrogen clusters stored in a binary clathrate hydrate, *Science*, *306*, 469–471.

Fukasawa, T., Y. Tominaga, and A. Wakisaka (2004), Molecular association in binary mixtures of tert-butyl alcohol-water and tetrahydrofuran-heavy water studied by mass spectrometry of clusters from liquid droplets, *J. Phys. Chem. A*, *108*, 59–63.

Gagnon, R. E., H. Kiefte, M. J. Clouter, and E. Whalley (1987), Elastic-constants of ice Ih, up to 2.8 kbar, by Brillouin spectroscopy, *J. Phys.*, *48*, 23–28.

Galashev, A. E., V. N. Chukanov, A. N. Novruzov, and O. A. Novruzova (2006), Molecular-dynamic calculation of spectral characteristics of absorption of infrared radiation by $(H_2O)(j)$ and $(CH_4)(i)(H_2O)(n)$ clusters, *High Temp.*, *44*, 364–372.

Handa, Y. P. (1984), Enthalpies of fusion and heat capacities for $H_2^{18}O$ ice and $H_2^{18}O$ tetrahydrofuran clathrate hydrate in the range 100–270 K, *Can. J. Chem.*, *62*, 1659–1661.

Handa, Y. P. (1986), Compositions, enthalpies of dissociations, and heat capacities in the range 85 to 270 K for clathrate hydrates of methane, ethane, and propane, and enthalpy of dissociation of isobutene hydrate as determined by a heat-flow calorimeter, *J. Chem. Thermodyn.*, *18*, 915–921.

Handa, Y. P. (1990), Effect of hydrostatic-pressure and salinity on the stability of gas hydrates, *J. Phys. Chem.*, *94*, 2652–2657.

Handa, Y. P., and D. Stupin (1992), Thermodynamic properties and dissociation characteristics of methane and propane hydrates in 70-angstrom-radius silica-gel pores, *J. Phys. Chem.*, *96*, 8599–8603.

Handa, Y. P., R. E. Hawkin, and J. J. Murray (1984), Calibration and testing of Tian-Calvet heat-flow calorimeter: Enthalpies of fusion and heat capacities for ice and tetrahydrofuran hydrate in the range 85 to 270 K, *J. Chem. Thermodyn.*, *16*, 623–632.

Helgerud, M. B., W. F. Waite, S. H. Kirby, and A. Nur (2003a), Measured temperature and pressure dependence of compressional (*Vp*) and shear (*Vs*) wave speeds in compacted, polycrystalline ice Ih, *Can. J. Phys.*, *81*, 81–87.

Helgerud, M. B., W. F. Waite, S. H. Kirby, and A. Nur (2003b), Measured temperature and pressure dependence of *Vp* and *Vs* in compacted, polycrystalline sI methane and sII methane-ethane hydrate, *Can. J. Phys.*, *81*, 47–53.

Hobbs, P. V. (1974), *Ice Physics*, 837 pp., Clarendon, Oxford, U. K.

Kiefte, H., M. J. Clouter, and R. E. Gagnon (1985), Determination of acoustic velocities of clathrate hydrates by Brillouin spectroscopy, *J. Phys. Chem.*, *89*, 3103–3108.

Leaist, D. G., J. J. Murray, M. L. Post, and D. W. Davidson (1982), Enthalpies of decomposition and heat-capacities of ethylene-oxide and tetrahydrofuran hydrates, *J. Phys. Chem.*, *86*, 4175–4178.

Lide, D. R. (Ed.) (2003), *CRC Handbook of Chemistry and Physics*, 2576 pp., CRC Press, Boca Raton, Fla.

Lin, W., G.-J. Chen, C.-Y. Sun, X.-Q. Guo, Z.-K. Wu, M.-Y. Liang, and L.-Y. Yang (2004), Effect of surfactant on the formation and dissociation kinetic behavior of methane hydrate, *Chem. Eng. Sci.*, *59*, 4449–4455.

Luck, W. A. P. (1973), Infrared studies of hydrogen bonding in pure liquids and solutions, in *Water: A Comprehensive Treatise*, edited by F. Franks, chap. 4, pp. 235–321, Springer, New York.

Masui, A., H. Haneda, Y. Ogata, and K. Aoki (2005), The effect of saturation degree of methane hydrate on the shear strength of synthetic methane hydrate sediments, in *Proceedings of Fifth International Conference on Gas Hydrates*, *Pap. 2037*, pp. 657–663, Tapir Acad., Trondheim, Norway.

Mitchell, J. K., and K. Soga (2005), *Fundamentals of Soil Behavior*, 592 pp., John Wiley, Hoboken, N. J.

Nishinaga, T., D. Yamazaki, H. Stahr, A. Wakamiya, and K. Komatsu (2003), Synthesis, structure, and dynamic behavior of cyclopentadienyl-lithium, -sodium, and -potassium annelated with bicyclo[2.2.2]octene units: A systematic study on site exchange of alkali metals on a cyclopentadienyl ring in tetrahydrofuran, *J. Am. Chem. Soc.*, *125*, 7324–7335.

Ohmura, R., T. Shigetomi, and Y. H. Mori (2002), Bending tests on clathrate hydrate single crystals, *Philos. Mag. A*, *82*, 1725–1740.

Ohtake, M., Y. Yamamoto, T. Kawamura, A. Wakisaka, W. F. de Souza, and A. M. V. de Freitas (2005), Clustering structure of aqueous solution of kinetic inhibitor of gas hydrates, *J. Phys. Chem. B*, *109*, 16,879–16,885.

Palomino, A. M., and J. C. Santamarina (2005), Fabric map for kaolinite: Effects of pH and ionic concentration on behavior, *Clays Clay Minerals*, *53*, 211–223.

Petrenko, V. F., and R. W. Whitworth (1999), *Physics of Ice*, 373 pp., Clarendon, Oxford, U. K.

Priest, J., A. Best, C. Clayton, and E. Watson (2005), Seismic properties of methane gas hydrate-bearing sand, in *Proceedings of Fifth International Conference on Gas Hydrates*, *Pap. 2007*, pp. 440–447, Tapir Acad., Trondheim, Norway.

Ross, R. G., P. Anderson, and G. Backstrom (1981), Unusual PT dependence of thermal conductivity for a clarthrate hydrate, *Nature*, *290*, 322–323.

Rueff, R. M., and E. D. Sloan (1985), Effect of granular sediment on some thermal properties of tetrahydrofuran hydrate, *Ind. Eng. Chem.*, *24*, 882–885.

Santamarina, J. C., K. A. Klein, and M. A. Fam (2001), *Soils and Waves*, 488 pp., John Wiley, Hoboken, N. J.

Santamarina, J. C., T. S. Yun, J. Y. Lee, A. Martin, F. Francisca, and C. Ruppel (2005), Mechanical, thermal and electromagnetic properties of hydrate-bearing clay, silt, and sand at various confining pressures, *Eos Trans. AGU*, *86*(47), Fall Meet. Suppl., Abstract OS41C-07.

Shi, W. X., B. L. Wang, and X. T. Li (2005), A measurement method of ice layer thickness based on resistance-capacitance circuit for closed loop external melt ice storage tank, *Appl. Therm. Eng.*, *25*, 1697–1707.

Sloan, E. D. (1998), *Clathrate Hydrates of Natural Gases*, 705 pp., CRC Press, Boca Raton, Fla.

Smallwood, I. M. (1996), *Handbook of Organic Solvent Properties*, 306 pp., Halsted, New York.

Spangenberg, E., and J. Kulenkampff (2005), Physical properties of gas hydrate bearing sediments, in *Proceedings of Fifth International Conference on Gas Hydrates*, *Pap. 2028*, pp. 587–596, Tapir Acad., Trondheim, Norway.

Spangenberg, E., J. Kulenkampff, R. Naumann, and J. Erzinger (2005), Pore space hydrate formation in a glass bead sample from methane dissolved in water, *Geophys. Res. Lett.*, *32*, L24301, doi:10.1029/2005GL024107.

Stern, L. A., S. H. Kirby, and W. B. Durham (1996), Peculiarities of methane clathrate hydrate formation and solid-state deformation, including possible superheating of water ice, *Science*, *273*, 1843–1848.

Takamuku, T., A. Nakamizo, M. Tabata, K. Yoshida, T. Yamaguchi, and T. Otomo (2003), Large-angle X-ray scattering, small-angle neutron scattering, and NMR relaxation studies on mixing states of 1,4-dioxane-water, 1,3-dioxane-water, and tetrahydrofuran-water mixtures, *J. Mol. Liquids*, *103*, 143–159, doi:10.1016/S0167–7322 (02)00133–2.

Uchida, T., T. Ebinuma, S. Takeya, J. Nagao, and H. Narita (2002), Effects of pore sizes on dissociation temperatures and pressures of methane, carbon dioxide, and propane hydrates in porous media, *J. Phys. Chem. B*, *106*, 820–826.

Upstill, C. E., and R. Evans (1977), Surface-tension and density profile of simple liquids, *J. Phys. C Solid State Phys.*, *10*, 2791–2799.

Valiullin, R., and I. Furo (2002), The morphology of coexisting liquid and frozen phases in porous materials as revealed by exchange of nuclear spin magnetization followed by H-1 nuclear magnetic resonance, *J. Chem. Phys.*, *117*, 2307–2316.

Waite, W. F., B. J. deMartin, S. H. Kirby, J. Pinkston, and C. D. Ruppel (2002), Thermal conductivity measurements in porous mixtures of methane hydrate and quartz sand, *Geophys. Res. Lett.*, *29*(24), 2229, doi:10.1029/2002GL015988.

Waite, W. F., W. J. Winters, and D. H. Mason (2004), Methane hydrate formation in partially water-saturated Ottawa sand, *Am. Mineral.*, *89*, 1202–1207.

Winters, W. J., I. A. Pecher, W. F. Waite, and D. H. Mason (2004), Physical properties of rock physics models of sediment containing natural and laboratory-formed methane gas hydrate, *Am. Mineral.*, *89*, 1221–1227.

Winters, W. J., L. Y. Gilbert, D. H. Mason, I. A. Pecher, and W. F. Waite (2005), Effect of grain size and pore pressure on acoustic and strength behavior of sediments containing methane gas hydrate, in *Proceedings of Fifth International Conference on Gas Hydrates*, *Pap. 2017*, pp. 507–516, Tapir Acad., Trondheim, Norway.

Yoshida, K., N. Tsuchihashi, K. Ibuki, and M. Ueno (2005), NMR and viscosity B coefficients for spherical nonelectrolytes in nonaqueous solvents, *J. Mol. Liquids*, *119*, 67–75.

Yun, T. S., F. M. Francisca, J. C. Santamarina, and C. Ruppel (2005), Compressional and shear wave velocities in uncemented sediment containing gas hydrate, *Geophys. Res. Lett.*, *32*, L10609, doi:10.1029/2005GL022607.

Yun, T. S., J. C. Santamarina, and C. Ruppel (2007), Mechanical properties of sand, silt, and clay containing tetrahydrofuran hydrate, *J. Geophys. Res.*, *112*, B04106, doi: 10.1029/2006JB004484.

Zakrzewski, M., and Y. P. Handa (1993), Thermodynamic properties of ice and of tetrahydrofuran hydrate in confined geometries, *J. Chem. Thermodyn.*, *25*, 631–637.

Zhong, Y., and R. E. Rogers (2000), Surfactant effects on gas hydrate formation, *Chem. Eng. Sci.*, *55*, 4175–4187.